AIAA SciTech Forum
11–15 & 19–21 January 2021, VIRTUAL EVENT
AIAA Scitech 2021 Forum

10.2514/6.2021-1830

State Space Modeling of Viscous Unsteady Aerodynamic Loads

Haithem E. Taha* and Amir S. Rezaei†
University of California, Irvine, CA 92697

In this paper, we started by summarizing our recently developed viscous unsteady theory based on coupling potential flow with the triple deck boundary layer theory. This approach provides a viscous extension of potential flow unsteady aerodynamics. As such, a Reynolds-number-dependence could be determined. We then developed a finite-state approximation of such a theory, presenting it in a state space model. This novel nonlinear state space model of the viscous unsteady aerodynamic loads is expected to serve aerodynamicists better than the classical Theodorsen's model, as it captures viscous effects (i.e., Reynolds number dependence) as well as nonlinearity and additional lag in the lift dynamics; and allows simulation of arbitrary time-varying airfoil motions (not necessarily harmonic). Moreover, being in a state space form makes it quite convenient for simulation and coupling with structural dynamics to perform aeroelasticity, flight dynamics analysis, and control design. We then proceeded to develop a linearization of such a model, which enables analytical results. So, we derived an analytical representation of the viscous lift frequency response function, which is an explicit function of, not only frequency, but also Reynolds number. We also developed a state space model of the linearized response. We finally simulated the nonlinear and linear models to a non-harmonic, small-amplitude pitching maneuver at $100,000$ **Reynolds number and compared the resulting lift and pitching moment with potential flow, in reference to relatively higher fidelity computations of the Unsteady Reynolds-Averaged Navier-Stokes equations.**

I. Introduction

The theory of two-dimensional unsteady aerodynamics has a long history that extends for a century. Perhaps the first formal efforts are those of Prandtl [1] and Birnbaum [2] in 1924, considering incompressible, slightly viscous flows around thin airfoils with sharp trailing edges. The key concept is that the flow nonuniformity leads to vorticity generation that emanate at the sharp trailing edge and freely shed behind the airfoil. In addition, the flow outside these sheets can be considered inviscid. As such, for example, the law of zero total circulation (consequence of the conservation of angular momentum in inviscid flows) can be used. These assumptions alone are not enough to determine a unique solution for the wing and wake circulations. Then, the Kutta-Zhukovsky condition (smooth flow off the sharp trailing edge) comes to play an essential role in the problem closure. That is, no flow around the sharp edge and hence, even within the framework of potential flow, the velocity has to be finite at the edge. Finally, in order to obtain an analytical explicit solution to the governing dynamics (the Laplace's equation in the velocity potential in this case), one more assumption is usually adopted. Assuming small disturbance to the mean flow so that the vorticity sheet would shed by the mean flow velocity (flat wake assumption) completes the framework of the classical theory. In summary, the classical theory of unsteady aerodynamics is based on replacing the airfoil and the wake by vorticity distributions (singularities) that satisfy the Laplace's equation everywhere in the flow field except at the surface of singularities. Three main conditions are applied: (1) no-penetration boundary condition (fluid velocity is parallel to the wing surface), (2) The Kutta condition (smooth flow off the sharp trailing edge), and (3) the conservation of total circulation ($\frac{D\Gamma}{Dt} = 0$). This formulation along with the flat wake assumption constitute the classical theory of unsteady aerodynamics.

The above formulation of the classical theory of unsteady aerodynamics was extensively used throughout the years. In 1925, Wagner [3] used this formulation to solve the indicial problem (lift response due to a step change in the angle of attack). In 1935, Theodorsen [4] used the same formulation to solve the frequency response problem (steady state lift response due to harmonic oscillation in the angle of attack). In 1938, Von Karman and Sears [5] provided a more general and elaborate representation of the classical formulation, which is of hitherto importance in developing extensions of the classical theory[6, 7]. Also, the efforts of Kussner [8] on the sharp edged gust problem, Schwarz [9] on the frequency response problem, Sears [10] on the sinusoidal gust problem, and Lowey [11] on the returning wake problem worth

*Associate Professor, Mechanical and Aerospace Engineering, AIAA Senior Member.
†Post Doctoral Fellow, Mechanical and Aerospace Engineering, AIAA Member.

mentioning. It should be noted that while the approaches within this framework may be different (i.e., different order of application of the boundary conditions and assumptions and different means of calculating the loads), these results are exactly equivalent. For example, Garrick [12] showed that the Theodorsen function and the Wagner function form a Fourier transform pair.

It should be pointed out that even with the several simplifying assumptions mentioned above (potential flow, flat wake, the Kutta assumption/condition, etc), the unsteady lift response of a two-dimensional airfoil is of an infinite dimensional nature. That is, in a dynamical-systems narrative, the lift transfer function has infinitely many poles [13]. The need for calculating the aerodynamic loads due to arbitrary time variations of the wing motion along with the need for structural and/or dynamic coupling to assess the aeroelastic and/or flight dynamic stability problems invoked more compact representations for the lift dynamics than the infinite-dimensional Theodorsen's and Wagner's responses. Consequently, a number of finite-state approximations to these response functions were developed. Jones [14] and Jones [15] provided a two-state approximation to the Wagner function in the time-domain. Vepa [16] introduced the method of Pade approximants to determine finite-state representations for the Theodorsen function in the frequency domain. Of particular interest to the aeroelasticity and flight dynamics community is the state space representation developed by Leishman and Nguyen [17] using the convolution integral with Jones approximation to the Wagner's step response function. Unlike these finite-state models that are based on approximating the Theodorsen function in the frequency domain or the Wagner function in the time domain, Peters and his colleagues derived state space models from the basic governing principles using Glauert expansion [18] or the expansion of potential functions [13, 19]. In this formulation, the internal aerodynamic states are of physical meaning; they represent the inflow distributions. Although the formulation of Peters is quite neat, it necessitates a relatively large number (eight) of inflow states to provide a good accuracy, whereas two states were shown to be sufficient for this problem. Recent efforts in developing state space models of unsteady aerodynamic loads include [20–23].

Having summarized the main results of the classical theory of unsteady aerodynamics, we should emphasize the following point: Insofar as Prandtl's potential-flow formulation was quite useful serving the community and even provides the basis for many recent developments [6, 7, 24–32], it is mainly based on inviscid flow dynamics; no regard can be given to a finite Reynolds number. More importantly, it is not complete and invokes a closure or auxiliary condition (e.g., the Kutta condition). This potential-flow formulation cannot *alone* determine the amount of shed vorticity at the trailing edge, which is a very crucial quantity as it determines the circulation bound the airfoil (via conservation of circulation), which in turn dictates the generated lift force. The most common auxiliary condition used in literature is the Kutta condition whose application to steady flows has been very successful. However, its application to unsteady flows has been controversial (see Crighton [33] and the references therein).

The need for an auxiliary condition alternative to Kutta's goes as early as the work of Howarth [34] with a research flurry on the applicability of Kutta condition to unsteady flows in the 1970's and 1980's [33, 35–38]. This research was mainly motivated by the failure to capture an accurate flutter boundary [39–41]. Since flutter simply lies in the intersection between unsteady aerodynamics and structural dynamics, and because the structural dynamics theory is in a much better status (vibration of slender beams can be accurately predicted using the exact beam theory for example), it has been deemed that the flaw stems from the classical unsteady aerodynamic theory, particularly the Kutta condition, as suggested by Chu [42] and Shen and Crimi [43] among others. Moreover, since these deviations occurred even at zero angle of attack (or lift) [44, 45], it was inferred that there is a fundamental issue with such a theory that is not merely a higher-order effect due to nonlinearities at high angles of attack [42]. Therefore, there was almost a consensus that the Kutta condition has to be relaxed particularly at large frequencies, large angles of attack and/or low Reynolds numbers [37, 46, 47]. In fact, Orszag and Crow [48] regarded the full-Kutta-condition solution as "indefensible". Interestingly, this dissatisfaction of the Kutta condition and the need for its relaxation is recently rejuvenated with the increased interests in the low Reynolds number, high frequency bio-inspired flight [6, 49–54]. For more recent discussion about the unsteady Kutta condition, the reader is referred to the efforts of Xia and Mohseni [55], Taha and Rezaei [56], and Zhu et al. [57].

We note that the whole issue about the Kutta condition stems from the fact that it provides a remedy for an inviscid theory of unsteady lift whereas the vorticity generation and lift development are essentially viscous processes. To relax the Kutta condition, we recently developed a viscous extension of the classical theory of unsteady aerodynamics [56], equivalently, an unsteady extension of the viscous boundary layer theory. It is based on a special boundary layer theory (the triple deck [58–60]) that pays close attention to the details in the vicinity of the trailing edge where the Blasius boundary layer [61] interacts with the Goldstein near wake layer [62]. Our viscous extension resulted in a Reynolds-number-dependent extension of Theodorsen's lift frequency response. It was found that the viscous correction induces a significant phase lag to the circulatory lift component, particularly at low Reynolds numbers and high

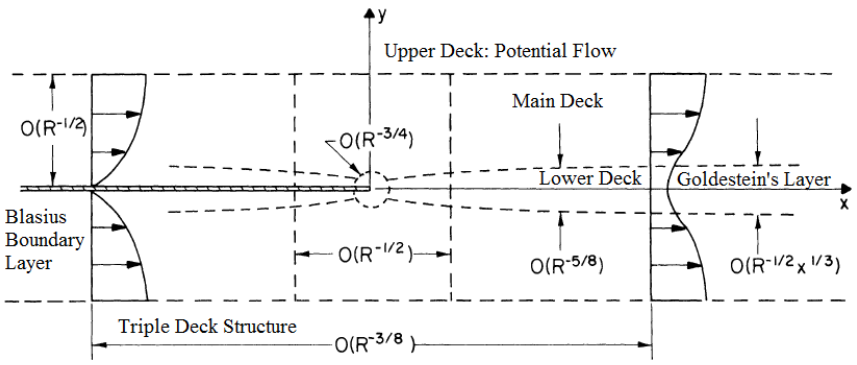

Fig. 1 Triple deck structure and various flow regimes. Adapted from Messiter [59].

frequencies, that matches high-fidelity simulations of Navier-Stokes and previous experimental results [38, 41, 45, 63].

In this paper, we summarize the developed viscous unsteady aerodynamic model. Based on which, we develop a nonlinear state space model for the viscous unsteady loads. We then linearize such a theory to determine an analytical representation, extending Theodorsen's lift frequency response function to the viscous case. That is, we provide an analytical lift frequency response function that explicitly depends, not only on the reduced frequency, but also on the Reynolds number. Similar to Theodorsen's, this viscous frequency response function is infinite-dimensional (i.e., has infinitely many poles). We then develop a finite state approximation of this infinite-dimensional viscous frequency response. That is, we provide a linearized state space model, extending that of Leishman and Nguyen [17] to the viscous case; the Reynolds number appears as a parameter in such a state space model. These tools will be of paramount importance in coupling viscous unsteady aerodynamics with structural dynamics for aeroelasticity and flight dynamics analysis as well as control synthesis.

II. A Viscous Theory of Unsteady Aerodynamics

A. Background: The Triple Deck Boundary Layer Theory

In the early 1900, Prandtl has formulated the well-known boundary layer equations [64]: the nonlinear partial differential equations that approximate Navier-Stokes equations in the thin viscous layer around the airfoil. In 1908, Blasius [61] solved this set of equations over a flat plate at zero angle of attack subject to the no-slip boundary condition on the plate, which lead to the celebrated Blasius boundary layer solution. Later (in 1930), Goldstein [62] solved the same boundary layer equations of Prandtl in the wake region behind the plate, replacing the no-slip condition with a zero-stress condition on the wake center line. He found that the removal of the wall accelerates the flow leading to a favorable pressure gradient. That is, near the trailing edge, there are two boundary layers interacting with each other, as shown in Fig. 1: the Blasius boundary layer, whose thickness is of order $R^{-1/2}$, and Goldstein near-wake, whose thickness is scaled as $R^{-1/2}x^{1/3}$ where R is the Reynolds number and x is the distance downstream of the edge [33]. The triple deck theory has been devised to model such local interactions near the trailing edge of a flat plate in steady flow. In contrast to the classical boundary layer theory where only the normal coordinate is scaled, the tangential coordinate is also scaled (zoomed) in the triple deck theory to resolve such interactions. Scaling dictates that the transition region between the two layers takes place over a short length of order $R^{-3/8}$ (as shown in Fig. 1), which is similar to Lighthill's supersonic shock-wave-boundary-layer interaction [65]. In conclusion, the triple deck theory represents a solution to the discontinuity of the viscous boundary condition at the edge [66]: from a zero tangential velocity on the airfoil to a zero pressure discontinuity on the wake center line.

Aerodynamicists modeled this transition through three decks (triple deck theory): (i) the upper deck which constitutes of an irrotational flow outside of the main boundary layer, (ii) the main deck which constitutes the main boundary layer (Blasius), and (iii) the lower deck, which is a sub-layer inside the main boundary layer, as shown in Fig. 1. Stewartson [58] and Messiter [59] were the first to develop the triple deck theory for a flat plate in a steady flow at zero angle of

attack. Their efforts resulted in the the following correction of the Blasius skin friction drag coefficient

$$C_D \simeq \frac{1.328}{\sqrt{Re}} + \frac{2.66}{Re^{7/8}},$$

which is in an astonishingly good agreement with both Navier-Stokes simulations and experiments down to $R = 10$ and even lower. Brown and Stewartson [60] extended the work of Stewartson [58] and Messiter [59] to the case of small but non-zero angle of attack α_s, in the order of $R^{-1/16}$. This range is of interest because (i) if α_s is much smaller, then the flow can be considered as a perturbation to the case of $\alpha_s = 0$ and (ii) if it is much larger, then the flow would separate well before the trailing edge. Over this range, the resulting adverse pressure gradient is of the same order as the favorable pressure gradient in the triple deck, leading to separation in the immediate vicinity of the trailing edge, which is called *Trailing Edge stall*. Brown and Stewartson [60] formulated such a problem and showed that the flow in the lower deck is governed by partial differential equations that are solved numerically for each value of $\alpha_e = R^{1/16}\lambda^{-9/8}\alpha_s$, where $\lambda = 0.332$ is the Blasius skin-friction coefficient. Chow and Melnik [67] solved the triple deck boundary layer equations in the case $0 < \alpha_e < 0.45$ and concluded that the flow will separate from the suction side of the airfoil from the trailing edge at $\alpha_e = 0.47$ (trailing edge stall angle). We remark that this α_e value for trailing edge stall corresponds to quite a small value for the actual angle of attack: $\alpha = 3.1^\circ - 4.2^\circ$ for $R = 10^4 - 10^6$.

Setting the axes at the center of the plate ($-1 \le \hat{x} \le 1$ on the plate), Brown and Stewartson [60] wrote the steady pressure distribution near the trailing edge ($\hat{x} = 1$) as

$$P_s(\hat{x} \to 1) = \rho U^2 \left[-\alpha_s \sqrt{\frac{1-\hat{x}}{2}} + \frac{B_s/2}{\sqrt{\frac{1-\hat{x}}{2}}} \right] \mathrm{sgn}(y), \tag{1}$$

where ρ is the fluid density, U is the free-stream, $\mathrm{sgn}(y)$ is positive on the upper surface, α is the angle of attack and B_s is the trailing edge singularity term, which is supposed to be zero according to the Kutta condition. In contrast, it is determined by matching the triple deck with the outer flow. The numerical solution by Chow and Melnik [67] provides B_e as a nonlinear function of α_e, which is represented here in Fig. 2(a), where

$$\alpha_e = \alpha_s \epsilon^{-1/2} \lambda^{-9/8} \quad \text{and} \quad B_s = 2\epsilon^3 \lambda^{-5/4} B_e(\alpha_e)\alpha_s, \tag{2}$$

where α_s, α_e are in radians, and $\epsilon = R^{-1/8} \ll 1$ [58]. In other words, Fig. 2(a) and Eq. (2) provide the trailing edge singularity B_s as a nonlinear function of the angle of attack α_s in a steady flow. Based on this theory, the Kutta steady lift can be corrected as

$$C_L = 2\pi \left(\sin \alpha_s - B_s \right), \tag{3}$$

which results in the viscous lift shown in Fig. 2(b) at different Reynolds numbers.

B. Viscous Unsteady Lift Frequency Response Using Triple Deck Theory

Brown and Daniels [66] were the first to extend the steady triple deck theory to the case of an oscillatory pitching flat plate. Unlike the steady case, there is a Stokes layer near the wall that is of order $\sqrt{\nu/\omega}$ where the viscous term is balanced by the time-derivative term in the equations. Brown and Daniels considered the impractical, yet mathematically-appealing, case of very high-frequency $k = O(R^{1/4}) = \frac{1}{\epsilon^2}$ and very small-amplitude $O(R^{-9/16})$, where k is the reduced frequency. Luckily, focusing on the more practical case of $0 < k << Re^{1/4}$ and $\alpha = O(R^{-1/16})$ results in vanishing the time-derivative term in both the main deck and lower deck equations, as shown by Brown and Cheng [68]. Therefore, the boundary layer equations look the same as those governing the steady case at a non-zero α_s (studied by Brown and Stewartson [60]) with a proper definition for the equivalent steady angle of attack. However, we emphasize that this approach is not a quasi-steady solution; although the time-derivative does not show up in the lower deck equations, the correspondence with the steady equations implies an equivalent angle of attack that is dependent on the oscillation frequency, as will be shown below. Therefore, the lower deck system is dynamical (i.e., possesses a non-trivial frequency response).

In our recent efforts [56, 69], we have developed a viscous extension of the classical theory of unsteady aerodynamics using the triple deck boundary layer theory discussed above. For an arbitrarily deforming thin airfoil in the presence of a uniform stream U, the inviscid pressure distribution is typically written as [70–72]

$$P(\theta, t) - P_\infty = \rho \left[\frac{1}{2} a_0(t) \tan \frac{\theta}{2} + \sum_{n=1}^{\infty} a_n(t) \sin n\theta \right], \tag{4}$$

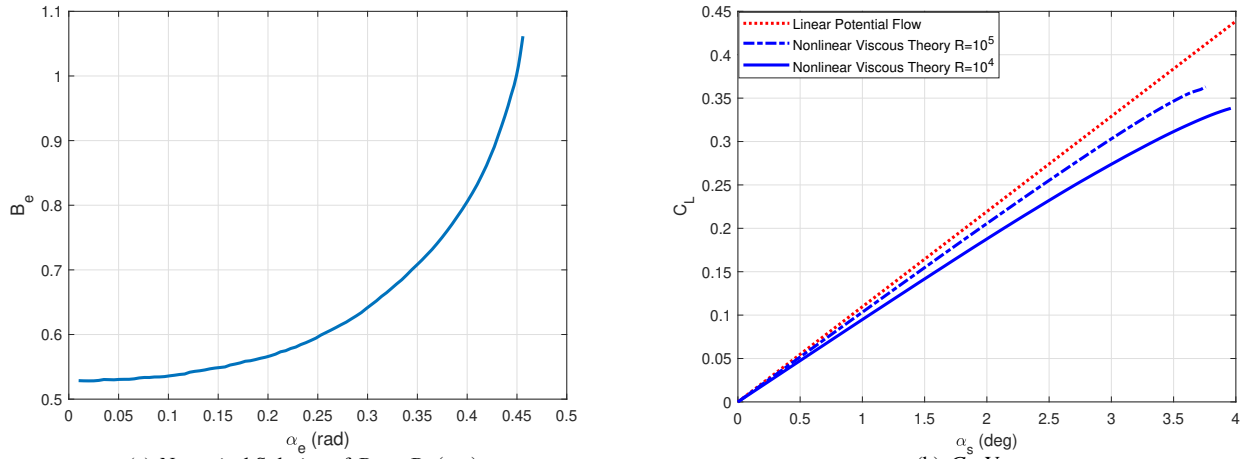

(a) Numerical Solution of $B_e = B_e(\alpha_e)$. (b) C_L Vs α.

Fig. 2 Chow and Melnik numerical solution of the steady lower deck equations for $0 < \alpha_e < 0.45$ [67] and the corresponding nonlinear viscous steady C_L-α curve at different Reynolds numbers.

where θ is the tangential angular coordinate along the plate (0 at trailing edge and π at the leading edge). Each term in the series (4) automatically satisfies the Kutta condition (zero loading at the trailing edge). The pressure on the lower side is given by the negative of Eq. (4). The no-penetration boundary condition provides a means to determine all the coefficients a_n's (except a_0) in terms of the plate motion kinematics, as shown by Robinson and Laurmann [72], pp. 491. For example, for a pitching-plunging flat plate, as shown in Fig. 3, the normal velocity of the plate is written as

$$v(x,t) = \dot{h}(t)\cos\alpha(t) - \dot{\alpha}(t)(x - ab) - U\sin\alpha(t), \quad -b \le x \le b, \tag{5}$$

where b is the half-chord length, h is the plunging displacement (positive upward), α is the pitching angle (angle of attack, positive clockwise), and ab represents the chordwise distance from the mid point to the hinge point, as shown in Fig. 3. This type of kinematics results in

$$a_1(t) = b\left(\dot{v}_{1/2}(t) - U\dot{\alpha}(t)\right), \quad a_2(t) = -\frac{b^2\ddot{\alpha}(t)}{4}, \quad \text{and} \quad a_n = 0 \ \forall n > 2, \tag{6}$$

where $v_{1/2}$ is the normal velocity at the mid-chord point, which is given by

$$v_{1/2}(t) = \dot{h}(t)\cos\alpha(t) + ab\dot{\alpha}(t) - U\sin\alpha(t).$$

The determination of a_0 (leading edge singularity term) is more involved in the sense that it requires solving an integral equation, which cannot be solved analytically for arbitrary time-varying wing motion. It has been solved for some common inputs, e.g., step change in the angle of attack resulting in the Wagner's response [3], simple harmonic motion resulting in Theodorsen's frequency response [4], sharp-edged gust resulting in Kussner's function [8], and sinusoidal gust resulting in Sears' function [10]. For example, the harmonic solution of Theodorsen implies [72], pp. 496

$$a_0 = U\left[2v_{3/4}C(k) + b\dot{\alpha}\right], \tag{7}$$

where $v_{3/4}$ is the normal velocity at the three-quarter-chord point, and $C(k)$ is the Theodorsen's frequency response function, which depends on the reduced frequency $k = \frac{\omega b}{U}$ as

$$C(k) = \frac{H_1^{(2)}(k)}{H_1^{(2)}(k) + iH_0^{(2)}(k)}, \tag{8}$$

where $H_n^{(m)}$ is the Hankel function of m^{th} kind of order n. Finally, the potential-flow lift force and pitching moment (positive pitching up) at the mid-chord point are written as

$$L_P = -\pi\rho b(a_0 + a_1) \quad \text{and} \quad M_{0_P} = \frac{\pi}{2}\rho b^2(a_2 - a_0). \tag{9}$$

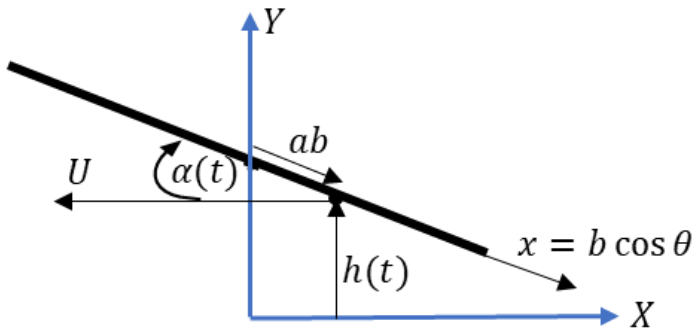

Fig. 3 A schematic diagram for an oscillating flat plate.

In the common classification proposed by Theodorsen [4], the terms proportional to $C(k)$ represent the circulatory contribution, while the other *algebraic* terms (i.e., free of dynamic lag), which are proportional to acceleration, represent the non-circulatory contribution [73, 74].

Relaxing the Kutta condition is equivalent to introducing an additional circulation Γ_{v} beyond Kutta's at the center of the cylinder, which induces singularities at the trailing and leading edges of the plate. Clearly, this circulation is of unknown strength; there is no means within potential flow for its determination. The Kutta condition dictates that it must vanish so as to remove the singularity at the trailing edge. However, we relax the Kutta condition and determine its dynamics via matching with the triple deck boundary layer theory. This additional circulation modifies the inviscid unsteady pressure distribution (4) as

$$P(\theta,t)-P_\infty=\rho\left[\frac{1}{2}a_0(t)\tan\frac{\theta}{2}+\sum_{n=1}^{\infty}a_n(t)\sin n\theta+\frac{1}{2}B_{\mathrm{v}}(t)\left(\cot\frac{\theta}{2}+a_{0_{\mathrm{v}}}(t)\tan\frac{\theta}{2}\right)\right], \tag{10}$$

where the correction B_{v} is related to the additional circulation as $B_{\mathrm{v}}=\frac{U\Gamma_{\mathrm{v}}}{2\pi b}$, and $a_{0_{\mathrm{v}}}$ is the leading edge singularity due to Γ_{v}. This term has a non-trivial dynamics (there is a non-trivial transfer function from Γ_{v} to $a_{0_{\mathrm{v}}}$). It can be determined from potential flow considerations: it is the a_0 term in the unsteady inviscid pressure distribution (4) over the plate due to a bound circulation Γ_{v}, ignoring the quasi-steady contribution (i.e., the wake effects only). Therefore, similar to the general a_0 term, it cannot be determined analytically for arbitrary kinematics; there is an analytical expression in the special case of harmonic motion ($a_{0_{\mathrm{v}}}=2C(k)-1$ [68]). In our recent effort [56], we used the unsteady triple deck theory, exploiting the vanishing of the time-derivative term from the boundary layer equations, to determine B_{v} in terms of k and R. Then, the viscous unsteady lift and pitching moment will be written as

$$L=-\pi\rho b\left(a_0+a_1+B_{\mathrm{v}}(1+a_{0_{\mathrm{v}}})\right)\quad\text{and}\quad M_0=\frac{\pi}{2}\rho b^2\left(a_2-a_0+B_{\mathrm{v}}(1-a_{0_{\mathrm{v}}})\right). \tag{11}$$

To determine the viscous correction B_{v} of the pressure distribution, consider approaching the trailing edge ($\theta\to 0$ or $\hat{x}=\frac{x}{b}\to 1$), the pressure distribution (10) is then written as

$$P(\hat{x}\to 1;t)-P_\infty=\rho\left[\left(\frac{1}{2}a_0(t)+2\sum_{n=1}^{\infty}na_n(t)+\frac{1}{2}B_{\mathrm{v}}(t)a_{0_{\mathrm{v}}}(t)\right)\sqrt{\frac{1-\hat{x}}{2}}+\frac{B_{\mathrm{v}}(t)/2}{\sqrt{\frac{1-\hat{x}}{2}}}\right], \tag{12}$$

which has the same form as the steady distribution given in Eq. (1) with

$$\alpha_s(t)\equiv\frac{1}{U^2}\left|\frac{1}{2}a_0(t)+2\sum_{n=1}^{\infty}na_n(t)\right|\quad\text{and}\quad B_{\mathrm{v}}(t)\equiv B_s=-2\epsilon^3\lambda^{-5/4}\left(\frac{1}{2}a_0(t)+2\sum_{n=1}^{\infty}na_n(t)\right)B_e(\alpha_e), \tag{13}$$

where α_s and B_s are the equivalent steady angle of attack and trailing edge singularity term, respectively. Note that the negligence of the term $B_{\mathrm{v}}a_{0_{\mathrm{v}}}$ when performing such an equivalence was justified in our earlier effort [56]. This

comparison along with the fact that the time-derivative term does not enter the triple deck equations is suggestive to utilize the steady solution by Chow and Melnik [67] of the inner deck equations for the unsteady case with the equivalence shown above, valid in the range $0 < k < O(R^{1/4})$. In the above equivalence, if the term $\frac{1}{2}a_0(t) + 2\sum_{n=1}^{\infty} n a_n(t)$ is negative, then the top of the oscillating thin airfoil will correspond to the top of the steady plate and if is positive, then the top of the oscillating thin airfoil should correspond to the bottom of the steady plate. In either case, α_s would be positive.

For a harmonically oscillating flat plate at a given reduced frequency k and Reynolds number R, the coefficients a_0, a_1, and a_2 of the inviscid pressure distribution are given in Eqs. (6,7). Thus, α_s can be obtained accordingly from Eq. (13). Care should be taken when applying Eq. (13). It should be applied instantaneously: at each time instant, the right hand side containing the a's coefficients is complex because a_0 contains the complex-valued function $C(k)$. The instantaneous $\alpha_s(t)$ should be given by

$$\alpha_s(t) = \frac{1}{U^2}\left|\Re\left[\frac{1}{2}a_0(t) + 2a_1(t) + 4a_2(t)\right]\right|,$$

where $\Re(.)$ denotes the real part of its complex argument. As such, the equivalent angle of attack $\alpha_e(t)$ for the numerical solution of Chow and Melnik [67] is obtained from Eq. (2) with $\epsilon = R^{-1/8}$. Note that if $\alpha_e(t)$ exceeds 0.47, then the simulation should be terminated because such a value implies trailing edge stall beyond which the current analysis is not valid. Using, Fig. 2(a), one can obtain $B_e(t)$, which in turn is substituted in Eq. (13) to determine the viscous correction $B_{\rm v}(t)$. Finally, the unsteady viscous lift and moment are written as

$$L = \underbrace{\underbrace{-\pi\rho b^2\dot{v}_{1/2}}_{\text{Non-circulatory}} \underbrace{-2\pi\rho U b v_{3/4}C(k)}_{\text{Circulatory}}}_{\text{Potential Flow Solution } L_P} \underbrace{-2\pi\rho b B_{\rm v} C(k)}_{\text{Viscous Correction}}, \tag{14}$$

This equation implies that the viscous contribution to the lift appears as a correction to the angle of attack $\alpha_{3/4} = -v_{3/4}/U$ at the three-quarter-chord point by an amount of $\tilde{B}_{\rm v} = \frac{B_{\rm v}}{U^2}$. That is, the viscous unsteady circulatory lift coefficient can be written as $C_{L_C} = 2\pi\left(\alpha_{3/4} - \tilde{B}_{\rm v}\right)C(k)$. Also, the pitching moment at the mid-chord point can also be written as

$$M_0 = -\pi\rho b^2\left[\underbrace{\frac{b^2}{8}\ddot{\alpha} + \frac{b}{2}U\dot{\alpha} + U v_{3/4}C(k)}_{\text{Potential Flow Solution } M_{0_P}} - \underbrace{B_{\rm v}(1 - C(k))}_{\text{Viscous Correction}}\right], \tag{15}$$

The viscous correction $B_{\rm v}C(k)$ to the unsteady circulatory lift is inherited in the pitching moment as well. However, there is an additional viscous correction to the pitching moment. As can be inferred from Eq. (11), the viscous lift contribution has two components: $B_{\rm v}a_{0_{\rm v}}$ acting at the quarter-chord point, similar to the inviscid circulatory lift; and $B_{\rm v}$ acting at the three-quarter-chord point. Hence, viscosity, not only induces lag to the circulatory lift [56], but also shifts the center of pressure; both effects are expected to impact the flutter boundary [75, 76].

III. Nonlinear State Space Model of Viscous Unsteady Loads

The above viscous unsteady model can be described by the block diagram shown in Fig. 4. Realizing that the two dynamic blocks represent potential-flow lift dynamics, we can construct a state space model for the viscous unsteady loads (i.e., for this block diagram) utilizing a proper finite state approximation of potential flow (e.g., Leishman and Nguyen [17] or Peters [13]).

Let the quadruple (A_P, B_P, C_P, D_P) represent a state space model of potential-flow lift dynamics (i.e., a state space representation of $C(k)$). Then, the corresponding transfer function must have a high-frequency gain of $\frac{1}{2}$, which implies that $D_p = \frac{1}{2}$ [74]. Also, the corresponding transfer function must have a unity dc gain. That is, if it is fed by say $v_{3/4}$, the output would be $v_{3/4}C(k)$ in the time domain (i.e., the unsteady version of $v_{3/4}$). Therefore, we can write

$$\begin{aligned} \dot{\chi}_1 &= [A_P]\chi_1 + [B_P]v_{3/4}, \\ y_P &= [C_P]\chi_1 + [D_P]v_{3/4}, \end{aligned} \tag{16}$$

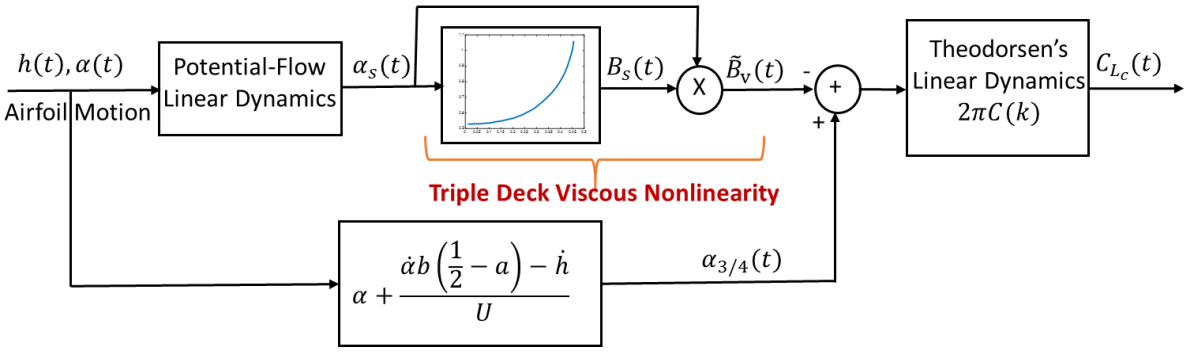

Fig. 4 A block diagram describing the dynamics of the viscous unsteady circulatory lift.

where $\chi_1 \in \mathbb{R}^n$ is the vector of internal aerodynamic states constituting the adopted potential-flow finite-state model of order n. The subscript 1 is used since another set of potential-flow states will be needed, as shown below. In this formulation, the output y_p represents $v_{3/4}C(k)$ in the time domain. As such, the potential-flow circulatory aerodynamic loads can be determined directly from y_P according to Eqs. (6-9) as

$$\begin{pmatrix} L_P \\ M_{0_P} \end{pmatrix}_C = -\pi\rho U b \begin{pmatrix} 2 \\ b \end{pmatrix} y_P \triangleq U[\mathbb{F}]y_P, \tag{17}$$

where $\mathbb{F}$ is the matrix (column) defining such a linear algebraic relation. In addition, the non-circulatory loads can be written in an abstract way as

$$\begin{pmatrix} L_P \\ M_{0_P} \end{pmatrix}_{NC} = [\mathbb{M}] \begin{pmatrix} \ddot{\alpha} \\ \ddot{h} \end{pmatrix} + [\mathbb{C}] \begin{pmatrix} \dot{\alpha} \\ \dot{h} \end{pmatrix}, \tag{18}$$

where the matrices $\mathbb{M}$ and $\mathbb{C}$ represent *added* mass and damping (actually the negative of mass and damping) induced by the non-circulatory loads, which are given by

$$\mathbb{M} = -\pi\rho b^2 \begin{bmatrix} ab & \cos\alpha \\ b^2/8 & 0 \end{bmatrix}, \quad \mathbb{C} = \pi\rho b^2 \begin{bmatrix} U\cos\alpha & \dot{\alpha}\sin\alpha \\ -Ub/2 & 0 \end{bmatrix}. \tag{19}$$

As such, the potential flow loads can be written in an abstract form as

$$\begin{pmatrix} L_P \\ M_{0_P} \end{pmatrix} = [\mathbb{M}] \begin{pmatrix} \ddot{\alpha} \\ \ddot{h} \end{pmatrix} + [\mathbb{C}] \begin{pmatrix} \dot{\alpha} \\ \dot{h} \end{pmatrix} + U[\mathbb{F}]y_P. \tag{20}$$

The block diagram shown in Fig. 4 implies that the sought state space model would include at least double the number n of the states constituting the adopted potential-flow finite-state model because it includes the potential-flow dynamics twice. In addition, to have a proper representation, we consider $\ddot{\alpha}$, $\ddot{h}$ to be the inputs to the aero dynamical system, hence, α, $\dot{\alpha}$, and $\dot{h}$ will be states. That is, the sought state space model would be of order $2n + 3$ whose state vector is $\chi = [\chi_1, \chi_2, \alpha, \dot{\alpha}, \dot{h}]^T$ and input vector is $u = [\ddot{\alpha}, \ddot{h}]^T$. As can be concluded from Eqs. (14,15), the potential-flow lift given above need to be corrected by adding terms proportional to B_v and $B_vC(k)$. The latter can be determined by passing the former to the potential flow state space representation (16).

To develop a state space representation for the viscous correction terms B_v and $B_vC(k)$, which is the main contribution of this work, we recall Eq. (13) and define the *effective* angle of attack

$$\alpha_{\text{eff}} = \frac{1}{U^2}\left[\frac{1}{2}a_0(t) + 2\sum_{n=1}^{\infty} n a_n(t)\right].$$

Note that this α_{eff} is different from the common notion of the effective angle of attack in potential flow. The former is a term special to the developed viscous theory, while the latter is simply given by the angle of attack $\alpha_{3/4}$ at the

three-quarter-chord point [70], pp. 80. Based on this definition, the equivalent steady angle of attack is simply given by $\alpha_s = |\alpha_{\text{eff}}|$. Then, we use Eqs. (6,7) to write α_{eff} as

$$\alpha_{\text{eff}} = \frac{v_{3/4}}{U} C(k) - \frac{3b\dot{\alpha}}{2U} + \frac{2b\dot{v}_{1/2} - b^2\ddot{\alpha}}{U^2}. \tag{21}$$

Realizing that $v_{3/4}C(k)$ is simply y_P, and substituting for $\dot{v}_{1/2}$, we write α_{eff} in terms of the states and inputs:

$$\begin{aligned} \alpha_{\text{eff}}(\chi;u) &= \frac{-1}{U}\begin{bmatrix} C_P & b\left(\frac{3}{2} + 2\cos\alpha + D_P(\frac{1}{2}-a)\right) & \frac{2b\dot{\alpha}}{U}\sin\alpha - D_P\cos\alpha \end{bmatrix}\begin{pmatrix} \chi_1 \\ \dot{\alpha} \\ \dot{h} \end{pmatrix} - D_P\sin\alpha + \\ &+ \frac{b}{U^2}\begin{bmatrix} (2a-1)b & 2\cos\alpha \end{bmatrix}\begin{pmatrix} \ddot{\alpha} \\ \ddot{h} \end{pmatrix}. \end{aligned} \tag{22}$$

As can be seen from Eq. (22), the effective angle of attack in the viscous theory depends on the accelerations. So, for relatively fast motion, α_{eff} reaches significant values, which trigger the nonlinearity of the $B_e(\alpha_e)$ curve (Fig. 2(a)), even with small amplitudes.

Having developed a state space representation of α_{eff} (and consequently α_s), Eq. (13) implies that the viscous correction B_{v} can be written in terms of the states and inputs as

$$B_{\text{v}}(\chi;u) = -2\epsilon^3\lambda^{-5/4}U^2\alpha_{\text{eff}}(\chi;u)B_e\left(\epsilon^{-1/2}\lambda^{-9/8}|\alpha_{\text{eff}}(\chi;u)|\right), \tag{23}$$

where $B_e(.)$ is a nonlinear function coming from the numerical solution of Chow and Melnik [67] to the triple deck problem, specifically from Fig. 2(a). Finally, the unsteady version of B_{v} (i.e., $B_{\text{v}}C(k)$) can be written with the aid of the potential-flow finite-state model (16) as

$$\begin{aligned} \dot{\chi}_2 &= [A_P]\chi_2 + [B_P]B_{\text{v}}, \\ y_{\text{v}} &= [C_P]\chi_2 + [D_P]B_{\text{v}}, \end{aligned} \tag{24}$$

where y_{v} simply represents $B_{\text{v}}C(k)$ in the time domain. The total viscous unsteady loads can then be written according to Eqs. (14,15) as

$$\begin{pmatrix} L \\ M_0 \end{pmatrix} = \begin{pmatrix} L_P \\ M_{0_P} \end{pmatrix} - \pi\rho b\begin{pmatrix} 2 \\ b \end{pmatrix}B_{\text{v}}C(k) + \pi\rho b^2\begin{pmatrix} 0 \\ 1 \end{pmatrix}B_{\text{v}}, \tag{25}$$

where the potential flow loads $\begin{pmatrix} L_P \\ M_{0_P} \end{pmatrix}$ are given by Eq. (20). Realizing that $\mathbb{F} = -\pi\rho b\begin{pmatrix} 2 \\ b \end{pmatrix}$ and that $B_{\text{v}}C(k)$ is y_{v}, which is given by Eq. (24), we finalize the state space model as follows. The state equation is written as

$$\begin{aligned} \frac{d}{dt}\begin{pmatrix} \chi_1 \\ \chi_2 \\ \alpha \\ \dot{\alpha} \\ \dot{h} \end{pmatrix} &= \begin{bmatrix} A_P & 0_{n\times n} & 0_{n\times 1} & -B_P b(\frac{1}{2}-a) & B_P\cos\alpha \\ 0_{n\times n} & A_P & 0_{n\times 1} & 0_{n\times 1} & 0_{n\times 1} \\ 0_{1\times n} & 0_{1\times n} & 0 & 1 & 0 \\ 0_{1\times n} & 0_{1\times n} & 0 & 0 & 0 \\ 0_{1\times n} & 0_{1\times n} & 0 & 0 & 0 \end{bmatrix}\begin{pmatrix} \chi_1 \\ \chi_2 \\ \alpha \\ \dot{\alpha} \\ \dot{h} \end{pmatrix} + \begin{pmatrix} -B_P U\sin\alpha \\ B_P B_{\text{v}}(\chi;u) \\ 0 \\ 0 \\ 0 \end{pmatrix} + \\ &+ \begin{bmatrix} 0_{n\times 1} & 0_{n\times 1} \\ 0_{n\times 1} & 0_{n\times 1} \\ 0 & 0 \\ 1 & 0 \\ 0 & 1 \end{bmatrix}\begin{pmatrix} \ddot{\alpha} \\ \ddot{h} \end{pmatrix} \end{aligned}, \tag{26}$$

where $B_{\text{v}}(\chi;u)$ is given in Eq. (23) in terms of the states $\chi = [\chi_1, \chi_2, \alpha, \dot{\alpha}, \dot{h}]^T$ and the inputs $u = [\ddot{\alpha}, \ddot{h}]^T$. The output

equation for the total viscous unsteady loads is then written as

$$\begin{pmatrix} L \\ M_0 \end{pmatrix} = \begin{bmatrix} U\mathbb{F}C_P & \mathbb{F}C_P & 0_{2\times1} & -UD_Pb(\frac{1}{2}-a)\mathbb{F}+\mathbb{C}(1) & UD_P\mathbb{F}\cos\alpha+\mathbb{C}(2) \end{bmatrix} \begin{pmatrix} \chi_1 \\ \chi_2 \\ \alpha \\ \dot{\alpha} \\ \dot{h} \end{pmatrix} + \\ + B_{\mathrm{v}}(\chi;u)\mathbb{F}' - U^2D_P\sin\alpha\mathbb{F} + \mathbb{M}\begin{pmatrix} \ddot{\alpha} \\ \ddot{h} \end{pmatrix}, \tag{27}$$

where $\mathbb{M}$ and $\mathbb{C}$ are defined in Eq. (19), $\mathbb{C}(j)$ is the j^{th} column of $\mathbb{C}$, and $\mathbb{F}' = D_p\mathbb{F} + \begin{pmatrix} 0 \\ \pi\rho b^2 \end{pmatrix}$.

The state space model presented in Eqs. (26,27) is simulated for the case of a pitching around the mid-chord point at $R = 10^5$, $k = 1$. The following non-harmonic waveform is used to demonstrate the power of the developed state space model in simulating arbitrary time-varying airfoil motion, in contrast to the frequency response model developed in our earlier effort [56]

$$\alpha(t) = A\left(e^{\sin\omega t} - 1\right), \tag{28}$$

where A is set to ensure that the maximum α throughout the cycle is 1°. Figure 5 shows the lift and pitching moment (at the mid-chord point) coefficients resulting from the state space model (26,27) in comparison to the potential flow simulation (i.e., $B_{\mathrm{v}} = 0$). Both results are compared in reference to the relatively higher fidelity simulations of the Unsteady Reynolds-Averaged Navier Stokes (URANS) equations, described in our earlier efforts [56, 77]. In simulating the viscous state space model (26,27), the following potential-flow finite-state model is adopted, which is similar to that of Leishman and Nguyen [78]:

$$A_P = \frac{U}{b}\begin{bmatrix} -b_1 & 0 \\ 0 & -b_2 \end{bmatrix},\ B_p = \frac{U}{b}\begin{pmatrix} b_1A_1 \\ b_2A_2 \end{pmatrix},\ C_P = \begin{bmatrix} 1 & 1 \end{bmatrix},\ D_P = 1 - A_1 - A_2,$$

where the constants A_1, A_2, b_1, b_2 are those defining Jones' two-state approximation [14]

$$\phi(s) = 1 - A_1e^{-b_1s} - A_2e^{-b_2s}$$

of the Wagner function, where $s = \frac{Ut}{b}$. Their values are: $A_1 = 0.165$, $A_2 = 0.335$, $b_1 = 0.0445$, and $b_2 = 0.3$.

Inspecting the results shown in Fig. 5, it is interesting to observe significant deviation from the classical potential-flow theory at this very small amplitude oscillations (maximum α is 1°). It is also interesting to report a very good matching between the computational results and the developed state space model. Indeed, it should serve aerodynamicists better than the classical Theodorsen's model, as it transcends the latter in the following aspects: (i) it provides viscous effects (i.e., Reynolds number dependence); (ii) it captures nonlinearity and additional lag in the lift dynamics due to viscosity, which will affect instability boundaries; (iii) it allows simulation of arbitrary time-varying airfoil motions (i.e., not confined to harmonic motions); (iv) being in a state space form makes it much more convenient than a frequency response function for simulation and coupling with structural dynamics to perform aeroelasticity, flight dynamics analysis, and control design; and (v) it is simply more accurate.

IV. Linearization of the Nonlinear Viscous Unsteady Theory

While the state space model (26,27) is indeed useful in simulation and analysis, it is always encouraging to seek analytical results. This goal is typically hard to achieve with a nonlinear theory, which invokes linearization of the nonlinear viscous unsteady theory developed above. Moreover, one drawback in the developed theory is its inability to tackle larger angles of attack; if α_e exceeds 0.47 (which corresponds to $\alpha \sim 3°$), the simulation must be terminated, which poses a good research problem on how to extend such a model, specifically Fig. (2(a)), to at least relatively larger angles of attack below stall (up to $\alpha \sim 10°$), perhaps by matching a given steady C_L-α curve [20, 79]. It should be noted that the classical inviscid theory (e.g., Theodrosen's model) suffers from the same issue of validity over a small α-range. Yet, it does not stipulate terminating the simulation if the angle of attack exceeds a certain value. Therefore, insofar as

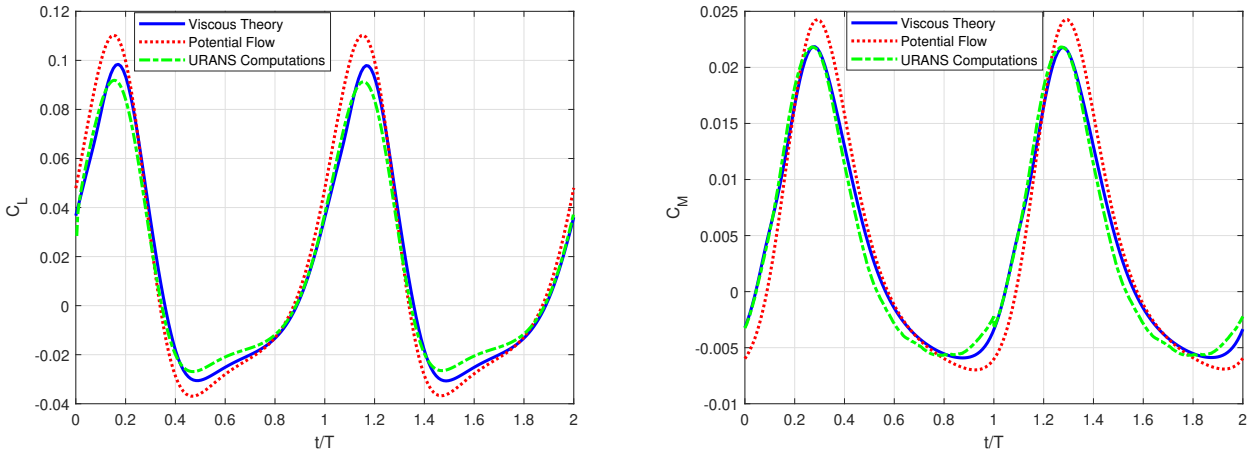

(a) Lift Response. (b) Pitching Moment Response.

Fig. 5 Response of the nonlinear state space model (26,27) of the viscous lift and pitching moment (at the mid-chord) to the non-harmonic pitching maneuver (28), in comparison to potential flow and URANS computations.

the inability to continue simulation of the developed theory is a limiting factor, it is an advantage beyond the classical theory in the sense that it precisely defines a region of applicability. Having said that, this issue will be circumvented any way in the linearized model below, realizing that linearization is typically valid for sufficiently small disturbances.

A. Analytical Representation of the Viscous Lift Frequency Response

It is indeed intriguing to develop an analytical representation of the viscous unsteady lift frequency response, similar to Theodorsen's, that depends not only on the frequency, but also on the Reynolds number. This goal is pursued below by simply linearizing the nonlinear viscous unsteady theory developed above.

Equation (25), or Eq. (14), implies

$$L = L_P - 2\pi\rho b B_{\mathrm{v}}.$$

The potential-flow lift L_P only possesses geometric nonlinearities, hence, it can be easily linearized, resulting in Theodrsen's transfer function of the circulatory lift. Therefore, the main nonlinearity in the developed theory of the viscous unsteady lift resides in B_{v}, which stems from the viscous triple deck boundary layer theory, as shown in the block diagram in Fig. 4. The B_{v}-contribution possesses two nonlinearities: the nonlinearity of the relation $B_e(\alpha_e)$ shown in Fig. 2(a); and a multiplicative nonlinearity represented by the term $\alpha_{\mathrm{eff}} \times B_e$ in Eq. (23). Expanding B_{v} in a Taylor series around the origin ($\chi = 0$, $u = 0$) and retaining only linear terms, we write

$$B_{\mathrm{v}}(\chi;u) \simeq B_{\mathrm{v}}(0;0) - 2\epsilon^3\lambda^{-5/4}U^2\left[\alpha_{\mathrm{eff}}(0;0)\Delta B_e\left(\alpha_e(0;0)\right) + B_e\left(\alpha_e(0;0)\right)\Delta\alpha_{\mathrm{eff}}(0;0)\right],$$

where Δ represents first-order variations. Equation (22) implies that $\alpha_{\mathrm{eff}}(0;0) = 0$, which results in zero α_s and α_e as well. This zero α_e, when plugged in the relation $B_e(\alpha_e)$ of Fig. 2(a), results in $B_e\left(\alpha_e(0;0)\right) \triangleq B_{e_0} = 0.53$. Moreover, the first-order variation of B_e at zero is almost zero; $B_e(\alpha_e)$ has an almost-zero slope at $\alpha_e = 0$. Hence, we have

$$B_{\mathrm{v}}(\chi;u) \simeq -2\epsilon^3\lambda^{-5/4}U^2 B_{e_0}\Delta\alpha_{\mathrm{eff}}(0;0).$$

Substituting the first variations of α_{eff} from Eq. (21), we obtain the following linearization of B_{v}

$$B_{\mathrm{v}}(\chi;u) \simeq -2\epsilon^3\lambda^{-5/4}B_{e_0}\left[U(\Delta v_{3/4})C(k) - \frac{3}{2}bU\dot{\alpha} + 2b\Delta\dot{v}_{1/2} - b^2\ddot{\alpha}\right], \tag{29}$$

where

$$\Delta v_{3/4} = \dot{h} - b(\frac{1}{2} - a)\dot{\alpha} - U\alpha, \quad \text{and} \quad \Delta\dot{v}_{1/2} = \ddot{h} + ab\ddot{\alpha} - U\dot{\alpha}. \tag{30}$$

Recalling the classification of lift in Eq. (14) and interpreting the viscous contribution as circulatory (since it is associated with an additional circulation); i.e., assuming the non-circulatory loads remain intact, the linearized viscous

circulatory lift is then written as

$$L_C = -2\pi\rho b\left[Uv_{3/4} - 2\epsilon^3\lambda^{-5/4}B_{e_0}\left(Uv_{3/4}C(k) - \frac{3}{2}bU\dot{\alpha} + 2b\dot{v}_{1/2} - b^2\ddot{\alpha}\right)\right]C(k). \tag{31}$$

Unlike the inviscid theory, there is no special point (e.g., the three-quarter-chord point) over the airfoil whose angle of attack solely dictates the circulatory lift. The lift response depends on the motion in a complicated way; it would not be possible to obtain a lift transfer function independent of kinematics. Nevertheless, we can derive analytical representations of the lift transfer function for harmonic pitching and plunging separately. In both cases, we define the viscous lift frequency response function C_{v}, similar to Theodorsen, as

$$C_{\mathrm{v}}(k;R) \triangleq \frac{L_C(k;R)}{L_{QS}(k)},$$

where L_{QS} is the quasi-steady lift given by $L_{QS} = -2\pi\rho bUv_{3/4}$.

1. Frequency Response due to Plunging

For a harmonic plunging motion $h(t) = He^{i\omega t}$, $v_{3/4} = \dot{h}$, and $\dot{v}_{1/2} = \ddot{h}$. As such, we obtain the viscous lift frequency response function

$$C_{\mathrm{v,Plunging}}(k;R) = \left[1 - 2R^{-3/8}\lambda^{-5/4}B_{e_0}\left(C(k) + 2ik\right)\right]C(k). \tag{32}$$

2. Frequency Response due to Pitching

For a harmonic pitching motion $\alpha(t) = A_\alpha e^{i\omega t}$, $v_{3/4} = -U\sin\alpha - \dot{\alpha}b(\frac{1}{2} - a)$, and $\dot{v}_{1/2} = ab\ddot{\alpha} - U\cos\alpha\dot{\alpha}$, resulting in

$$\Delta v_{3/4}(k) = -UA_\alpha\left[1 + ik(\frac{1}{2} - a)\right], \quad \text{and} \quad \Delta\dot{v}_{1/2}(k) = -\frac{U^2}{b}A_\alpha\left[ak^2 + ik\right]$$

As such, we obtain the viscous lift frequency response function

$$C_{\mathrm{v,Pitching}}(k;R) = \left[1 - 2R^{-3/8}\lambda^{-5/4}B_{e_0}\left(C(k) + \frac{\frac{7}{2}ik - (1-2a)k^2}{1 + ik(1/2 - a)}\right)\right]C(k). \tag{33}$$

Equations (32,32) represent, for the first time, analytical representations of the viscous lift frequency response. That is, one can account for the Reynolds-number-dependence in an explicit way. Clearly, as $R \to \infty$, both $C_{\mathrm{v}} \to C(k)$; one recovers the inviscid behavior as Reynolds number approaches infinity. Therefore, these two functions may replace the Theodorsen function in the future analysis. Figure 6 shows the variations of these two viscous lift frequency response functions with reduced frequency at different Reynolds numbers, in comparison to the inviscid response of Theodorsen. While the theory does not predict a considerable change in the magnitude of the transfer function from the inviscid response, it predicts a significant deviation in phase; the larger the frequency and the lower the Reynolds number, the larger the deviation in phase from Theodorsen's phase. These results were observed in our earlier effort [56] using a describing function analysis of the nonlinear theory. They are also captured here by the simple analytical relations (32,32). For a discussion about the physical reason behind this viscosity-induced lag and its relation to the Kutta condition, the reader is referred to our earlier effort [56].

The obtained phase results are also in accordance with the experimental results of Chu and Abramson [45], Henry [41], Abramson and Ransleben [63], and Bass et al. [38]. In these experimental efforts, the authors reconciled the deviation between Theodorsen's prediction of the unsteady aerodynamic loads and their measurements by adding some suggested phase lag to Theodorsen function, which is naturally captured in the developed viscous theory. For example, Chu and Abramson [45] suggested adding a phase lag of -10° to Theodorsen function for a better estimate of the unsteady lift and flutter boundary when $k \simeq 0.5$. Bass et al. [38] conducted a water tunnel experiment for a NACA 16-012 undergoing pitching oscillations around its quarter-chord point in the range of $0.5 < k < 10$ and $R = 6,500 - 26,500$. They compared their force measurements to Theodorsen's potential flow frequency response. They found bad agreement in the range $0.5 < k < 2$ where the most pronounced boundary layer activity is observed and the flow near the trailing edge is separating and alternating around the trailing edge. They concluded that adding a phase lag of -30° to the Theodorsen's $C(k)$ would make the predicted lift from the classical theory of unsteady aerodynamics

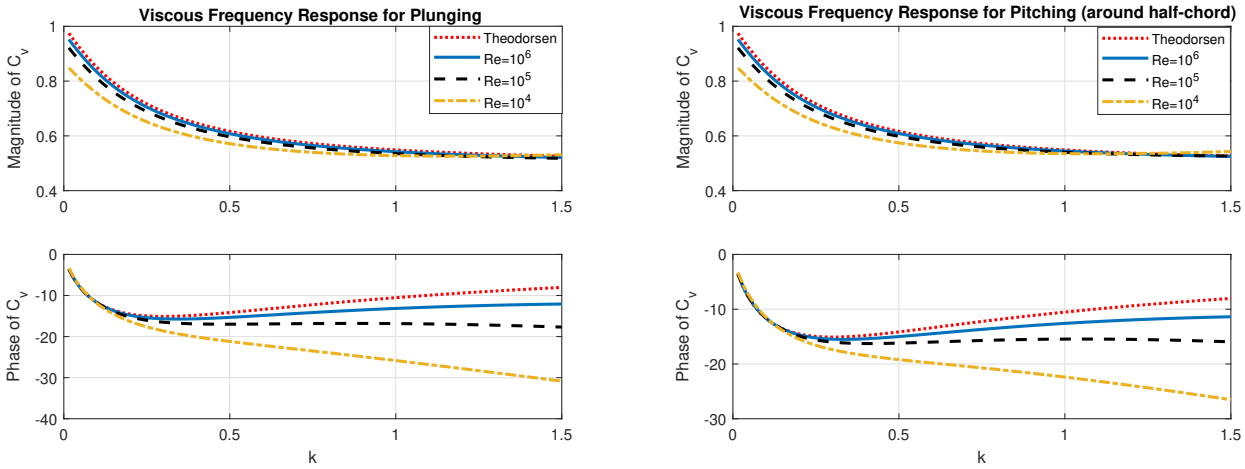

(a) Plunging.

(b) Pitching around the mid-chord point.

Fig. 6 Variation of the viscous lift frequency response with Reynolds number in the case of plunging and pitching (around the mid-chord) in comparison to the inviscid response of Theodorsen.

match their experimental measurements over this range. Similarly, there are several efforts in literature that suggest adding phase lag to Theodorsen's inviscid frequency response. However, there was no theoretical model that could predict the appropriate phase lag at a given combination of frequency and Reynolds number. The developed viscous unsteady theory fills this gap by providing a reasonable estimate of such a phase lag. This result is particularly important for flutter calculation. Note that the flutter instability, similar to any typical hopf bifurcation, is mainly dictated by when energy is added/subtracted during the cycle. That is, the phase difference between the applied loads (aerodynamic loads) and the system motion (e.g., angle of attack) plays a crucial role in dictating the stability boundary. Therefore, if Theodorsen's model does not capture such a phase lag accurately, it may lead to a deviation in the flutter boundary. As such, it is expected that the developed viscous frequency response will result in a more accurate, yet efficient, estimate of the flutter boundary.

Finally, it may be interesting to discuss the following point. Unlike the pitching case, where it is hard to interpret the $\dot{\alpha}$-terms in the viscous correction as circulatory or non-circulatory (since both contributions in potential flow include $\dot{\alpha}$-terms), such a classification is straight forward in the plunging case. In this case, the total viscous unsteady lift can be written as

$$L = \underbrace{\underbrace{-\pi\rho b^2\dot{v}_{1/2}}_{\text{Non-circulatory}}\ \underbrace{-2\pi\rho bUv_{3/4}C(k)}_{\text{Circulatory}}}_{\text{Inviscid}} \underbrace{-2R^{-3/8}\lambda^{-5/4}B_{e_0}\left(-2\pi\rho bUv_{3/4}C^2(k) - 4\pi\rho b^2\dot{v}_{1/2}\right)}_{\text{Viscous}},$$

which suggests classifying the $v_{3/4}$-term in the viscous contribution as circulatory and the $\dot{v}_{1/2}$-term as non-circulatory (added-mass). Doing so, we obtain a viscous frequency response of the circulatory lift as $C_{\text{v}}(k;R) = \left[1 - 2R^{-3/8}\lambda^{-5/4}B_{e_0}C(k)\right]C(k)$, simultaneously with a viscous (i.e., Reynolds-number-dependent) added-mass that is also frequency-dependent:

$$m_{\text{v}}(k;R) = \pi\rho b^2\left[1 - 8R^{-3/8}\lambda^{-5/4}B_{e_0}C(k)\right]. \tag{34}$$

Following this classification, the resulting viscous frequency response C_{v} of the circulatory lift is quite close to Theodorsen's. That is, the main viscous contribution actually resides in the acceleration term, which explains why the viscous response deviates from Theodorsen's response at higher frequencies. Therefore, this discussion suggests that, for pure plunging, one can model the viscous effects by just considering the modified (decreased) frequency-dependent added mass m_{v} given in Eq. (34).

B. Analytical Linear State Space Representation of Viscous Unsteady Loads

Since the nonlinear state space model (26,27) is valid only for small angles, it may be prudent to develop a linearized version of it. Having linearized the viscous frequency response theory, developed earlier [56], to obtain the analytical

frequency response functions (32,32), it should be straight forward to linearize the nonlinear state space model (26,27). The geometric nonlinearities in the model (26,27) can be easily linearized; the main non-trivial nonlinear term is B_{v}, which has been already linearized above, as given in Eq. (29) in the frequency domain. Therefore, it can be written in the time domain as

$$B_{\mathrm{v}}(\chi;u) \simeq -2\epsilon^3\lambda^{-5/4}B_{e_0}\left[Uy_P - \frac{7}{2}bU\dot{\alpha} + 2b\ddot{h} - (1-2a)b^2\ddot{\alpha}\right],$$

where y_P is the output from the potential-flow state space model (16); i.e., the time-domain version of $v_{3/4}C(k)$. Substituting y_P from Eq. (16), and the linearized $v_{3/4}$ from Eq. (30), then B_{v} can be written linearly in the states in the time-domain as

$$B_{\mathrm{v}}(\chi;u) \simeq -R_L\left[U\left(C_P\chi_1 + D_PH_{3/4}\chi_3\right) - \frac{7}{2}bU\dot{\alpha} + 2b\ddot{h} - (1-2a)b^2\ddot{\alpha}\right], \tag{35}$$

where $R_L = 2R^{-3/8}\lambda^{-5/4}B_{e_0}$ is a constant (related to the effect of the Reynolds number R on lift), χ_3 is the third set of states: $\chi_3 = [\alpha, \dot{\alpha}, \dot{h}]^T$, and $H_{3/4}$ defines the linear dependence of $v_{3/4}$ on χ_3:

$$\Delta v_{3/4} = \begin{bmatrix} -U & -b(\frac{1}{2}-a) & 1 \end{bmatrix}\begin{pmatrix} \alpha \\ \dot{\alpha} \\ \dot{h} \end{pmatrix} \triangleq H_{3/4}\chi_3 \tag{36}$$

As such, the nonlinear state space model (26,27) can then be linearized into the following form

$$\begin{aligned} \frac{d}{dt}\begin{pmatrix} \chi_1 \\ \chi_2 \\ \chi_3 \end{pmatrix} &= \begin{bmatrix} A_P & 0_{n\times n} & B_PH_{3/4} \\ -UR_LB_PC_P & A_P & -UR_LD_PB_PH_{3/4} \\ 0_{3\times n} & 0_{3\times n} & 0_{3\times 3} \end{bmatrix}\begin{pmatrix} \chi_1 \\ \chi_2 \\ \chi_3 \end{pmatrix} + \\ &+ \begin{bmatrix} 0_{n\times 1} & 0_{n\times 1} & 0_{n\times 1} \\ \frac{7}{2}UbR_LB_P & (1-2a)b^2R_LB_P & -2bR_LB_P \\ & I_{3\times 3} & \end{bmatrix}\begin{pmatrix} \dot{\alpha} \\ \ddot{\alpha} \\ \ddot{h} \end{pmatrix}, \end{aligned} \tag{37}$$

and the output equation can be written in the linear form

$$\begin{aligned} \begin{pmatrix} L \\ M_0 \end{pmatrix} &= \begin{bmatrix} U(\mathbb{F}-R_LD_p\mathbb{F}')C_P & \mathbb{F}C_P & UD_P(\mathbb{F}-R_LD_p\mathbb{F}')H_{3/4} \end{bmatrix}\begin{pmatrix} \chi_1 \\ \chi_2 \\ \chi_3 \end{pmatrix} + \\ &- \frac{\pi}{2}\rho Ub^2\begin{pmatrix} -2(1-7R_LD_p) \\ b[1-7R_L(1-D_P)] \end{pmatrix}\dot{\alpha} + \mathbb{M}_{\mathrm{v}}\begin{pmatrix} \ddot{\alpha} \\ \ddot{h} \end{pmatrix}, \end{aligned} \tag{38}$$

where $\mathbb{M}_{\mathrm{v}}$ represents the viscous version of the mass matrix $\mathbb{M}$, and is given by

$$\mathbb{M}_{\mathrm{v}} = -\pi\rho b^2\begin{bmatrix} b[a+2R_LD_p(1-2a)] & 1-4R_LD_p \\ b^2[\frac{1}{8}-R_L(1-2a)(1-D_P)] & 2R_Lb(1-D_P) \end{bmatrix}. \tag{39}$$

Figure 7 shows the simulation of the linearized viscous state space model (37,38) subject to the non-harmonic, small-amplitude maneuver defined in Eq. (28). As expected, for small-amplitude maneuvers such as the one considered here, the response of the linearized viscous system matches well that of the nonlinear system (26,27); both match the higher-fidelity URANS simulations. As such, the simple four-state ($2n$) system (37,38) is expected to be of a significant benefit to aeroelasticians and flight dynamicists, as it captures viscous unsteady effects in a convenient dynamical system form (state space form), allowing efficient simulation and coupling with structural dynamics for linear stability analysis (e.g., flutter analysis) and control design.

V. Conclusion

In this paper, we developed a nonlinear state space model of the viscous unsteady aerpdynamic loads. The model presents a finite-state approximation of the recently developed viscous unsteady aerodynamic theory that couples

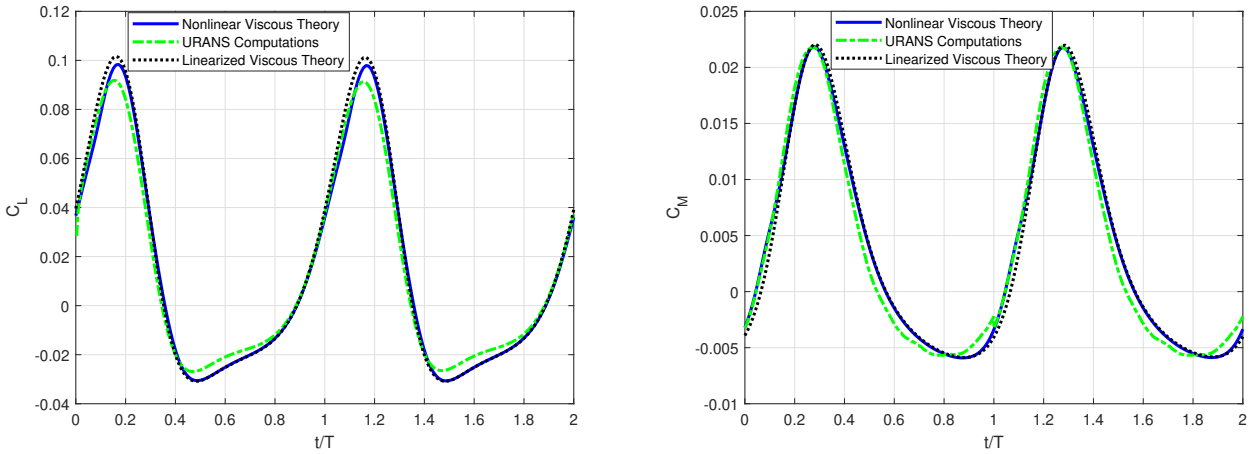

(a) Lift Response. (b) Pitching Moment Response.

Fig. 7 Response of the linear state space model (37,38) of the viscous lift and pitching moment (at the mid-chord) to the non-harmonic pitching maneuver (28), in comparison to the nonlinear model (26,27) and URANS computations.

potential flow with the triple deck boundary layer theory. The model consists of four internal aerodynamic states. It is validated against relatively higher-fidelity computations of the Unsteady Reynolds-Averaged Navier Stokes (URANS) equations. Comparisons show that the potential-flow results could deviate significantly from the viscous theory even for a very small-amplitude oscillation (down to 1°). Moreover, the developed nonlinear state space model is in a very good agreement with the URANS predictions of lift and moment over a specified range of angle of attack. Therefore, this model will be of paramount importance to aeroelasticians and flight dynamicists since (i) it captures viscous Reynolds number effects including nonlinearity and additional lag in the lift dynamics; (ii) it allows simulation of arbitrary time-varying maneuvers (not necessarily harmonic); and (iii) being in a state-space form, it allows straight forward coupling with structural dynamics for aeroelasticity and flight dynamics analysis and control design. Moreover, linearizing such a theory, we derived a linear state space model and an analytical representation of the viscous lift frequency response function, which is an explicit function of, not only the frequency, but also the Reynolds number.

VI. Acknowledgments

The authors would like to acknowledge the support of the National Science Foundation grant CBET-2005541.

References

[1] Prandtl, L., "Über die Entstehung von Wirbeln in der idealen Flüssigkeit, mit Anwendung auf die Tragflügeltheorie und andere Aufgaben," *Vorträge aus dem Gebiete der Hydro-und Aerodynamik (Innsbruck 1922)*, Springer, 1924, pp. 18–33.

[2] Birnbaum, W., "Der Schlagflugelpropeller und die Kleinen Schwingungen elastisch befestigter Tragfluegel," *Z Flugtech Motorluftschiffahrt*, Vol. 15, 1924, pp. 128–134.

[3] Wagner, H., "Uber die entstehung des dynamischen auftriebs von tragflugeln," *ZAMM*, Vol. 5, 1925.

[4] Theodorsen, T., "General Theory of Aerodynamic Instability and the Mechanism of Flutter," Tech. Rep. 496, NACA, 1935.

[5] Von Karman, T., and Sears, W. R., "Airfoil theory for non-uniform motion." *J. Aeronautical Sciences*, Vol. 5, No. 10, 1938, pp. 379–390.

[6] Ansari, S. A., Żbikowski, R., and Knowles, K., "Non-linear unsteady aerodynamic model for insect-like flapping wings in the hover. Part 1: methodology and analysis," *Proceedings of the Institution of Mechanical Engineers, Part G: Journal of Aerospace Engineering*, Vol. 220, No. 2, 2006, pp. 61–83.

[7] Tchieu, A. A., and Leonard, A., "A discrete-vortex model for the arbitrary motion of a thin airfoil with fluidic control," *Journal of Fluids and Structures*, Vol. 27, No. 5, 2011, pp. 680–693.

[8] Küssner, H. G., "Schwingungen von Flugzeugflügeln," *Jahrbuch der deutscher Versuchsanstalt für Luftfahrt especially Section E3 Einfluss der Baustoff-Dämpfung*, 1929, pp. 319–320.

[9] Schwarz, L., "Brechnung der Druckverteilung einer harmonisch sich Verformenden Tragflache in ebener Stromung," Luftfahrtforsch, 1940.

[10] Sears, W. R., "Some aspects of non-stationary airfoil theory and its practical application," *Journal of the Aeronautical Sciences*, Vol. 8, No. 3, 1941, pp. 104–108.

[11] Loewy, R. G., "A two-dimensional approximation to unsteady aerodynamics in rotary wings," *Journal of Aeronautical Sciences*, Vol. 24, 1957, pp. 81–92.

[12] Garrick, I. E., "On some reciprocal relations in the theory of nonstationary flows," Tech. Rep. 629, NACA, 1938.

[13] Peters, D. A., "Two-dimensional incompressible unsteady airfoil theory—An overview," *Journal of Fluids and Structures*, Vol. 24, 2008, pp. 295–312.

[14] Jones, R. T., "Operational treatment of the nonuniform lift theory to airplane dynamics," Tech. Rep. 667, NACA, 1938.

[15] Jones, W. P., "Aerodynamic forces on wings in non-uniform motion," Tech. Rep. 2117, British Aeronautical Research Council, 1945.

[16] Vepa, R., "On the use of Pade approximants to represent unsteady aerodynamic loads for arbitrarily small motions of wings," AIAA-Paper 1976-17, 1976.

[17] Leishman, J. G., and Nguyen, k. Q., "State-Space Representation of Unsteady Airfoil Behavior," *AIAA Journal*, Vol. 28, No. 5, 1990, pp. 836–844.

[18] Peters, D. A., and Karunamoorthy, S., "State-space inflow models for rotor aeroelasticity," AIAA-paper 1994-1920-CP, 1994.

[19] Peters, D. A., Karunamoorthy, S., and Cao, W., "Finite-state induced flow models, Part I: two-dimensional thin airfoil." *Journal of Aircraft*, Vol. 44, 1995, pp. 1–28.

[20] Taha, H., Hajj, M. R., and Beran, P. S., "State Space Representation of the Unsteady Aerodynamics of Flapping Flight," *Aerospace Science and Technology*, Vol. 34, 2014, pp. 1–11.

[21] Zakaria, M. Y., Taha, H., Hajj, M. R., and Hussein, A. A., "Experimental-Based Unified Unsteady Nonlinear Aerodynamic Modeling For Two-Dimensional Airfoils," AIAA-Paper 2015-3167, 2015.

[22] Zakaria, M. Y., Taha, H., and Hajj, M. R., "Measurement and Modeling of Lift Enhancement on Plunging Airfoils: A Frequency Response Approach," *Journal of Fluids and Structures*, Vol. 69, 2017, pp. 187–208.

[23] dos Santos, C. R., Pacheco, D. R. Q., Taha, H. E., and Zakaria, M. Y., "Nonlinear modeling of electro-aeroelastic dynamics of composite beams with piezoelectric coupling," *Composite Structures*, 2020, p. 112968.

[24] Jones, M. A., "The separated flow of an inviscid fluid around a moving flat plate," *Journal of Fluid Mechanics*, Vol. 496, 2003, pp. 405–441.

[25] Yongliang, Y., Binggang, T., and Huiyang, M., "An analytic approach to theoretical modeling of highly unsteady viscous flow excited by wing flapping in small insects," *Acta Mechanica Sinica*, Vol. 19, No. 6, 2003, pp. 508–516.

[26] Pullin, D. I., and Wang, Z., "Unsteady forces on an accelerating plate and application to hovering insect flight," *Journal of Fluid Mechanics*, Vol. 509, 2004, pp. 1–21.

[27] Michelin, S., and Smith, S. G. L., "An unsteady point vortex method for coupled fluid–solid problems," *Theoretical and Computational Fluid Dynamics*, Vol. 23, No. 2, 2009, pp. 127–153.

[28] Wang, C., and Eldredge, J. D., "Low-order phenomenological modeling of leading-edge vortex formation," *Theoretical and Computational Fluid Dynamics*, Vol. 27, No. 5, 2013, pp. 577–598.

[29] Ramesh, K., Gopalarathnam, A., Edwards, J. R., Ol, M. V., and Granlund, K., "An unsteady airfoil theory applied to pitching motions validated against experiment and computation." *Theoretical and Computational Fluid Dynamics*, 2013, pp. 1–22.

[30] Ramesh, K., Gopalarathnam, A., Granlund, K., Ol, M. V., and Edwards, J. R., "Discrete-vortex method with novel shedding criterion for unsteady aerofoil flows with intermittent leading-edge vortex shedding," *Journal of Fluid Mechanics*, Vol. 751, 2014, pp. 500–538.

[31] Yan, Z., Taha, H., and Hajj, M. R., "Geometrically-Exact Unsteady Model for Airfoils Undergoing Large Amplitude Maneuvers," *Aerospace Science and Technology*, Vol. 39, 2014, pp. 293–306.

[32] Li, J., and Wu, Z.-N., "Unsteady lift for the Wagner problem in the presence of additional leading/trailing edge vortices," *Journal of Fluid Mechanics*, Vol. 769, 2015, pp. 182–217.

[33] Crighton, D. G., "The Kutta condition in unsteady flow," *Annual Review of Fluid Mechanics*, Vol. 17, No. 1, 1985, pp. 411–445.

[34] Howarth, L., "The theoretical determination of the lift coefficient for a thin elliptic cylinder," *Proceedings of the Royal Society of London. Series A, Mathematical and Physical Sciences*, Vol. 149, No. 868, 1935, pp. 558–586.

[35] Basu, B. C., and Hancock, G. J., "The unsteady motion of a two-dimensional aerofoil in incompressible inviscid flow," *Journal of Fluid Mechanics*, Vol. 87, No. 01, 1978, pp. 159–178.

[36] Daniels, P. G., "On the unsteady Kutta condition," *The Quarterly Journal of Mechanics and Applied Mathematics*, Vol. 31, No. 1, 1978, pp. 49–75.

[37] Satyanarayana, B., and Davis, S., "Experimental studies of unsteady trailing-edge conditions," *AIAA Journal*, Vol. 16, No. 2, 1978, pp. 125–129.

[38] Bass, R. L., Johnson, J. E., and Unruh, J. F., "Correlation of lift and boundary-layer activity on an oscillating lifting surface," *AIAA Journal*, Vol. 20, No. 8, 1982, pp. 1051–1056.

[39] Rott, N., and George, M. B. T., "An Approach to the Flutter Problem in Real Fluids," Tech. Rep. 509, 1955.

[40] Abramson, H. N., and Chu, H.-H., "A discussion of the flutter of submerged hydrofoils," *Journal of Ship Research*, Vol. 3, No. 2, 1959.

[41] Henry, C. J., "Hydrofoil Flutter Phenomenon and Airfoil Flutter Theory," Tech. Rep. 856, Davidson Laboratory, 1961.

[42] Chu, W.-H., "An aerodynamic analysis for flutter in Oseen-type viscous flow," *Journal of the Aerospace Sciences*, Vol. 29, 1961, pp. 781–789.

[43] Shen, S. F., and Crimi, P., "The theory for an oscillating thin airfoil as derived from the Oseen equations," *Journal of Fluid Mechanics*, Vol. 23, No. 03, 1965, pp. 585–609.

[44] Woolston, D. S., and Castile, G. E., "Some effects of variations in several parameters including fluid density on tbe flutter speed of light uniform cantilever wings," Tech. Rep. 2558, NACA, 1951.

[45] Chu, W.-H., and Abramson, H. N., "An Alternative Formulation of the Problem of Flutter in Real Fluids," *Journal of the Aerospace Sciences*, Vol. 26, No. 10, 1959.

[46] Abramson, H. N., Chu, W.-H., and Irick, J. T., "Hydroelasticity with special reference to hydrofoil craft." Tech. Rep. 2557, NSRDC Hydromechanics Lab, 1967.

[47] Savage, S. B., Newman, B. G., and Wong, D. T.-M., "The role of vortices and unsteady effects during the hovering flight of dragonflies," *The Journal of Experimental Biology*, Vol. 83, No. 1, 1979, pp. 59–77.

[48] Orszag, S. A., and Crow, S. C., "Instability of a Vortex Sheet Leaving a Semi-Infinite Plate," *Studies in Applied Mathematics*, Vol. 49, No. 2, 1970, pp. 167–181.

[49] Ansari, S. A., Zbikowski, R., and Knowles, K., "Non-linear Unsteady Aerodynamic Model for Insect-Like Flapping Wings in the Hover. Part2: Implementation and Validation," *Journal of Aerospace Engineering*, Vol. 220, 2006, pp. 169–186.

[50] Pitt Ford, C. W., and Babinsky, H., "Lift and the leading-edge vortex," *Journal of Fluid Mechanics*, Vol. 720, 2013, pp. 280–313.

[51] Hemati, M. S., Eldredge, J. D., and Speyer, J. L., "Improving vortex models via optimal control theory," *Journal of Fluids and Structures*, Vol. 49, 2014, pp. 91–111.

[52] Zakaria, M. Y., Taha, H. E., and Hajj, M. R., "Design Optimization of Flapping Ornithopters: The Pterosaur Replica in Forward Flight," *Journal of Aircraft*, , No. DOI: 10.2514/1.C033154, 2015.

[53] Hussein, A. A., Seleit, A. E., Taha, H. E., and Hajj, M. R., "Optimal transition of flapping wing micro-air vehicles from hovering to forward flight," *Aerospace Science and Technology*, Vol. 90, 2019, pp. 246–263.

[54] Al-Haik, M. Y., Zakaria, M. Y., Hajj, M. R., and Haik, Y., "Storage of energy harvested from a miniature turbine in a novel organic capacitor," *Journal of Energy Storage*, Vol. 6, 2016, pp. 232–238.

[55] Xia, X., and Mohseni, K., "Unsteady aerodynamics and vortex-sheet formation of a two-dimensional airfoil," *Journal of Fluid Mechanics*, Vol. 830, 2017, pp. 439–478.

[56] Taha, H., and Rezaei, A. S., "Viscous Extension of Potential-Flow Unsteady Aerodynamics: The Lift Frequency Response Problem," *Journal of Fluid Mechanics*, Vol. 868, 2019, pp. 141–175. doi:10.1017/jfm.2019.159.

[57] Zhu, W., McCrink, M. H., Bons, J. P., and Gregory, J. W., "The unsteady Kutta condition on an airfoil in a surging flow," *Journal of Fluid Mechanics*, Vol. 893, 2020.

[58] Stewartson, K., "On the flow near the trailing edge of a flat plate," *Proceedings of the Royal Society of London A: Mathematical, Physical and Engineering Sciences*, Vol. 306, No. 1486, 1968, pp. 275–290.

[59] Messiter, A. F., "Boundary-layer flow near the trailing edge of a flat plate," *SIAM Journal on Applied Mathematics*, Vol. 18, No. 1, 1970, pp. 241–257.

[60] Brown, S. N., and Stewartson, K., "Trailing-edge stall," *Journal of Fluid Mechanics*, Vol. 42, No. 03, 1970, pp. 561–584.

[61] Blasius, H., *Grenzschichten in Flüssigkeiten mit kleiner Reibung*, Druck von BG Teubner, 1908.

[62] Goldstein, S., "Concerning some solutions of the boundary layer equations in hydrodynamics," *Mathematical Proceedings of the Cambridge Philosophical Society*, Vol. 26, No. 1, 1930, pp. 1–30.

[63] Abramson, H. N., and Ransleben, G. E., "An experimental investigation of flutter of a fully submerged subcavitating hydrofoil," *Journal of Aircraft*, Vol. 2, No. 5, 1965, pp. 439–442.

[64] Schlichting, H., Gersten, K., Krause, E., Oertel, H., and Mayes, K., *Boundary-layer theory*, Vol. 7, Springer, 1955.

[65] Lighthill, M. J., "On boundary layers and upstream influence. II. Supersonic flows without separation," *Proceedings of the Royal Society of London A: Mathematical, Physical and Engineering Sciences*, Vol. 217, The Royal Society, 1953, pp. 478–507.

[66] Brown, S. N., and Daniels, P. G., "On the viscous flow about the trailing edge of a rapidly oscillating plate," *Journal of Fluid Mechanics*, Vol. 67, No. 04, 1975, pp. 743–761.

[67] Chow, R., and Melnik, R. E., "Numerical solutions of the triple-deck equations for laminar trailing-edge stall," *Proceedings of the Fifth International Conference on Numerical Methods in Fluid Dynamics June 28–July 2, 1976 Twente University, Enschede*, Springer, 1976, pp. 135–144.

[68] Brown, S. N., and Cheng, H. K., "Correlated unsteady and steady laminar trailing-edge flows," *Journal of Fluid Mechanics*, Vol. 108, 1981, pp. 171–183.

[69] Taha, H., and Rezaei, A. S., "Unsteady Viscous Lift Frequency Response Using The Triple Deck Theory," AIAA-Paper 2018-0038, 2018.

[70] Schlichting, H., and Truckenbrodt, E., *Aerodynamics of the Airplane*, McGraw-Hill, 1979.

[71] Bisplinghoff, R. L., Ashley, H., and Halfman, R. L., *Aeroelasticity*, Dover Publications, New York, 1996.

[72] Robinson, A., and Laurmann, J. A., *Wing theory*, Cambridge University Press, 1956.

[73] Taha, H., and Rezaei, A. S., "On the Dynamics of Unsteady Lift and Circulation and the Circulatory-Non-circulatory Classification," AIAA-Paper 2019-1853, 2019.

[74] Taha, H., and Rezaei, A. S., "On the High-Frequency Response of Unsteady Lift and Circulation: A Dynamical Systems Perspective," Vol. 93, 2020, p. 102868.

[75] Taha, H., and Rezaei, A. S., "Effect of Viscous Unsteady Aerodynamics on Flutter Calculation," AIAA-Paper 2019-2036, 2019.

[76] Zakaria, M. Y., Al-Haik, M. Y., and Hajj, M. R., "Experimental analysis of energy harvesting from self-induced flutter of a composite beam," *Applied Physics Letters*, Vol. 107, No. 2, 2015, p. 023901.

[77] Rezaei, A. S., and Taha, H., "Computational Study of Lift Frequency Responses of Pitching Airfoils at Low Reynolds Numbers," AIAA-Paper 2017-0716, 2017.

[78] Leishman, J. G., and Beddoes, T. S., "A Semi-Empirical Model for Dynamic Stall," *J. the American Helicopter Soc.*, Vol. 34, No. 3, 1989, pp. 3–17.

[79] Taha, H., Hajj, M. R., and Beran, P. S., "Unsteady Nonlinear Aerodynamics of Hovering MAVs/Insects," AIAA-Paper 2013-0504, 2013.